

NEUROTRANSMITTER RECEPTOR DENSITY CHANGES IN *PITX3*^{AK} MICE – A MODEL RELEVANT TO PARKINSON'S DISEASE

J. N. CREMER,^{a,b*} K. AMUNTS,^{a,c} J. GRAW,^d M. PIEL,^e
F. RÖSCH^e AND K. ZILLES^{a,b}

^a Institute of Neuroscience and Medicine (INM-1), Research Center Jülich, D-52425 Jülich, Germany

^b Department of Psychiatry, Psychotherapy and Psychosomatics, University Hospital, RWTH Aachen University, and JARA – Translational Brain Medicine, D-52062 Aachen, Germany

^c Cécile & Oskar Vogt Institute of Brain Research, Heinrich-Heine University Düsseldorf, University Hospital Düsseldorf, Moorenstr. 5, D-40225 Düsseldorf, Germany

^d Helmholtz Center Munich, Institute of Developmental Genetics (IDG), Ingolstaedter Landstraße 1, D-85764 Neuherberg, Germany

^e Institute of Nuclear Chemistry, Johannes Gutenberg University of Mainz, Fritz-Strassmann-Weg 2, D-55128 Mainz, Germany

Abstract—Parkinson's disease (PD) is the second most common neurodegenerative disorder, characterized by alterations of nigrostriatal dopaminergic neurotransmission. Compared to the wealth of data on the impairment of the dopamine system, relatively limited evidence is available concerning the role of major non-dopaminergic neurotransmitter systems in PD. Therefore, we comprehensively investigated the density and distribution of neurotransmitter receptors for glutamate, GABA, acetylcholine, adrenaline, serotonin, dopamine and adenosine in brains of homozygous *aphakia* mice being characterized by mutations affecting the *Pitx3* gene. This genetic model exhibits crucial hallmarks of PD on the neuropathological, symptomatic and pharmacological level. Quantitative receptor autoradiography was used to characterize 19 different receptor binding sites in eleven brain regions in order to understand receptor changes on a systemic level. We demonstrated striking differential changes of neurotransmitter receptor densities for numerous receptor types and brain regions, respectively. Most prominent, a strong up-regulation of GABA receptors and associated benzodiazepine binding sites in different brain regions and concomitant down-regulations of striatal nicotinic acetylcholine and serotonergic receptor densities were found. Furthermore, the densities of glutamatergic kainate, muscarinic acetylcholine, adrenergic α_1 and dopaminergic D₂/D₃ receptors were differentially altered. These results present novel insights into the expression of neurotransmitter receptors in *Pitx3*^{ak} mice supporting findings on PD pathology in patients and indicating on the possible

underlying mechanisms. The data suggest *Pitx3*^{ak} mice as an appropriate new model to investigate the role of neurotransmitter receptors in PD. Our study highlights the relevance of non-dopaminergic systems in PD and for the understanding of its molecular pathology.

© 2014 IBRO. Published by Elsevier Ltd. All rights reserved.

Key words: Parkinson's disease, *Pitx3*^{ak}, neurotransmitter receptor, mouse model.

INTRODUCTION

Neurotransmitter receptors are major targets for pharmaceutical intervention in neurological and psychiatric disorders, since alterations of neurotransmitter systems are often found in such diseases of humans as well as in respective animal models (Zilles et al., 1999; Cremer et al., 2009; Palomero-Gallagher et al., 2009, 2012). In Parkinson's disease (PD), the dominant role of changes in dopaminergic neurotransmission, resulting from degeneration of dopamine producing neurons in the substantia nigra is well known. This deficit can be compensated for a considerable but limited time by application of the dopamine precursor L-DOPA. However, the possible involvement of non-dopaminergic transmitter systems and their receptors is poorly understood, though studies indicate that changes regarding the glutamatergic, GABAergic, acetylcholinergic, adrenergic, serotonergic and adenosine system play a role in PD pathogenesis (de Jong et al., 1984; Tohgi et al., 1993; Rodriguez et al., 1998; Kerenyi et al., 2003; Kas et al., 2009; Varani et al., 2010).

The *aphakia* mouse (gene symbol *ak*) has been extensively studied as a model for abnormal lens development (Grimm et al., 1998; Graw, 1999; Rieger et al., 2001). Molecularly, it is characterized by two major deletions in the promoter of the *Pitx3* gene. Therefore, we here refer to this mutant as *Pitx3*^{ak} mice (Semina et al., 2000; Ahmad et al., 2013). Moreover, it has been described that these mice exhibit a selective and severe loss of dopaminergic neurons in the substantia nigra (Hwang et al., 2003; Nunes et al., 2003; van den Munckhof et al., 2003; Smidt et al., 2004), establishing *Pitx3*^{ak} as a model relevant to PD. The nigral cell loss entails a reduction of dopaminergic innervation in the striatum (van den Munckhof et al., 2003). At the motor level, *Pitx3*^{ak} mice exhibit deficits in striatum-dependent cognitive and nigrostriatal pathway-sensitive behavioral tests,

*Correspondence to: J. N. Cremer, Institute of Neuroscience and Medicine (INM-1), Research Center Jülich, D-52425 Jülich, Germany. Tel: +49-2461-61-1939.

E-mail address: je.cremer@fz-juelich.de (J. N. Cremer).

Abbreviations: 6-OHDA, 6-hydroxydopamine; ANOVA, analysis of variance; MPTP, 1-methyl-4-phenyl-1,2,3,6-tetrahydropyridin; NMDA, N-methyl-D-aspartate; PD, Parkinson's disease; ROI, regions of interest.

reflected by impairments concerning rotarod learning, t-maze performance, inhibitory avoidance tasks, challenging beam and pole test (Hwang et al., 2005; Ardayfio et al., 2008). These motor deficits can be reversed by L-DOPA treatment (Hwang et al., 2005; van den Munckhof et al., 2006), which in case of chronic administration leads to L-DOPA-induced dyskinesia (Ding et al., 2007). Taken together, *Pitx3^{ak}* mice represent a rodent model of PD, exhibiting crucial hallmarks at the neuro-pathological, symptomatic and pharmacological level.

To shed light on the role of dopaminergic and non-dopaminergic neurotransmitter receptors in PD and enlarge our knowledge of potential targets for intervention, we comprehensively analyzed the density and distribution of 19 different binding sites for glutamate, GABA, acetylcholine, adrenaline, serotonin, dopamine and adenosine in *Pitx3^{ak}* mice brains. Besides the classical motor symptoms caused by altered nigrostriatal neurotransmission, PD patients exhibit several non-motor symptoms, e.g. neuropsychiatric and cognitive deficits, autonomic, sensory and sleep disorders (Ziemssen and Reichmann, 2007; Lohle et al., 2009; Park and Stacy, 2009). Therefore, we focused our approach on eleven different brain regions relevant for motor- (i.e., cerebellum, striatum, substantia nigra and motor cortex) and non-motor function (i.e., olfactory bulb; somatosensory, piriform and visual cortices; hippocampal regions CA1, CA2/3 and dentate gyrus).

EXPERIMENTAL PROCEDURES

Materials

[³H]AMPA, [³H]kainate, [³H]MK 801, [³H]muscimol, [³H]SR 95531, [³H]flumazenil, [³H]pirenzepine, [³H]oxotremorine-M, [³H]AF-DX 384, [³H]4-DAMP, [³H]jepibatidine, [³H]prazosin, [³H]UK14,304, [³H]8-OH-DPAT, [³H]ketanserin, [³H]SCH 23390 and [³H]raclopride were purchased from Perkin Elmer, Rodgau, Germany. [³H]CGP 54626, [³H]LY 341495 and [³H]ZM 241385 were purchased from Biotrend, Cologne, Germany. [³H]fallypride was synthesized in our laboratory. Briefly, norfallypride (N-((1-allylpyrrolidin-2-yl)methyl)-5-(3-fluoropropyl)-2-hydroxy-3-methoxybenzamide) was dissolved in DMF and labeled at room temperature using [³H]methyl nosylate and Cs₂CO₃. Purification of the crude product via semi-preparative HPLC gave [³H]fallypride in a radiochemical yield of 69%, a radiochemical purity of >99.5%, and a specific activity of 1406 GBq/mmol.

Animals

Mice were kept under specific pathogen-free conditions at the Helmholtz Center Munich. For this study, homozygous male *Pitx3^{ak}* mice of 4–6 months of age (*n* = 12) and corresponding C57Bl/6 control mice (*n* = 6) were used. Former studies have shown that a number of six animals is a sufficient group size for autoradiographic analysis in case of well-established control mice strains like C57Bl/6 (Zilles et al., 2000; Oermann et al., 2005; Cremer et al., 2011). The size of the *Pitx3^{ak}* group was larger than that of the control group

to compensate for potentially higher interindividual differences and receive statistical reliable results. Experiments were performed according to the German animal welfare act and approved by the responsible governmental agency, LANUV NRW (Regional authorities for nature, environment and consumer protection NRW). Mice (28 ± 3 g bodyweight) were anesthetized using CO₂ and subsequently decapitated. After immediate removal of the brains, the brains were frozen in isopentane and stored at –80 °C.

Tissue processing

Unfixed, frozen brains were serially sectioned (10 μm at –15 °C) in the coronal plane using a cryostat (Leica Mikrosysteme Vertrieb GmbH, Mikroskopie und Histologie, Wetzlar, Germany). Alternating sections were mounted on pre-cooled, gelatin-coated glass slides, dried on a heating plate and either processed for quantitative *in vitro* receptor autoradiography according to standard protocols (Zilles et al., 2002a,b, 2004; Palomero-Gallagher et al., 2003) or histological cresyl violet staining, respectively. Slices were stored in vacuum-sealed plastic boxes at –80 °C.

Receptor autoradiography

Nineteen different receptor binding sites of the neurotransmitters glutamate (AMPA, kainate, N-methyl-D-aspartate (NMDA), mGlu2/3), GABA (GABA_A, GABA_B, benzodiazepine binding sites BZ), acetylcholine (M₁, M₂, M₃, nicotinic), noradrenaline (α₁, α₂), serotonin (5-HT_{1A}, 5-HT₂), dopamine (D₁, D₂/D₃), and adenosine (A_{2A}) were analyzed after incubating the brain slices in solutions containing the respective tritiated ligands. The procedure has been previously described in detail (Zilles et al., 2002a,b). Briefly, the autoradiographic labeling method consists of three steps: (1) the preincubation for rehydrating the sections and removing endogenous ligand, (2) the main incubation for labeling of receptors with the tritiated ligand in the absence (total binding) or presence (nonspecific binding) of a specific non-radioactive displacer, and (3) the washing step for elimination of unbound ligand as well as buffer salts. Detailed incubation protocols are summarized in Table 1, including receptor subtypes, ³H-ligands, non-radioactive displacers, buffer compositions, incubation and washing times.

Image analysis

Radioactively labeled sections were co-exposed with plastic standards of known radioactivity concentrations against β-sensitive films (Kodak, PerkinElmer LAS GmbH, Germany) for nine to fifteen weeks, depending on the respective tritiated ligand. The sections of control and *Pitx3^{ak}* mice for each given ligand were exposed for exactly the same amount of time, which was nine weeks in case of [³H]LY 341495, [³H]CGP 54626, [³H]flumazenil, [³H]AF-DX 384 or [³H]4-DAMP binding, twelve weeks for [³H]kainate, [³H]MK 801, [³H]muscimol, [³H]SR 95531 and [³H]pirenzepine and 15 weeks in case of [³H]AMPA, [³H]oxotremorine-M, [³H]jepibatidine,

Table 1. Summary of receptor subtypes, ³H-ligands, non-radioactive displacers and incubation conditions of the autoradiographic experiments

Receptor	³ H-ligand, amount in main incubation	Displacer, amount in main incubation	Incubation buffer	Preincubation	Main incubation	Rinsing
AMPA	AMPA, 10 nM	Quisqualate, 10 μM	50 mM Tris–acetate (pH 7.2), 100 mM KSCN ^a	3 × 10 min, 4 °C	45 min, 4 °C	4 × 4 s, 4 °C; 2 × 2 s in 2.5% glutaraldehyde in acetone
Kainate	Kainate, 9.4 nM	SYM 2081, 100 μM	50 mM Tris–citrate (pH 7.1), 10 mM Calcium acetate ^a	3 × 10 min, 4 °C	45 min, 4 °C	3 × 4 s, 4 °C; 2 × 2 s in 2.5% glutaraldehyde in acetone
NMDA	MK 801, 3.3 nM	MK 801, 100 μM	50 mM Tris–HCl (pH 7.2), 50 μM Glutamate, 30 μM Glycine ^a , 50 μM Spermidine ^a	15 min, 4 °C	60 min, 22 °C	2 × 5 min, 4 °C; 1 s in distilled water
mGlu2/3	LY 341495, 1 nM	L–Glutamate, 1 mM	Phosphate-buffer (pH 7.6) 137 mM NaCl, 2.7 mM KCl, 4.3 mM Na ₂ HPO ₄ × 2H ₂ O, 1.4 mM KH ₂ PO ₄ , 100 mM KBr ^a	2 × 5 min, 22 °C	60 min, 4 °C	2 × 5 min, 4 °C; 1 s in distilled water
GABA _A	Muscimol, 7.7 nM	GABA, 10 μM	50 mM Tris–citrate (pH 7.0)	3 × 5 min, 4 °C	40 min, 4 °C	3 × 3 s, 4 °C; 1 s in distilled water
GABA _A	SR 95531, 3 nM	GABA, 1 mM	50 mM Tris–citrate (pH 7.0)	3 × 5 min, 4 °C	40 min, 4 °C	3 × 3 s, 4 °C; 1 s in distilled water
GABA _B	CGP 54626, 2 nM	CGP 55845, 100 μM	50 mM Tris–HCl (pH 7.2), 2.5 mM CaCl ₂	3 × 5 min, 4 °C	60 min, 4 °C	3 × 2 s, 4 °C; 1 s in distilled water
BZ	Flumazenil, 1 nM	Clonazepam, 2 μM	170 mM Tris–HCl (pH 7.4)	15 min, 4 °C	60 min, 4 °C	2 × 1 min, 4 °C; 1 s in distilled water
M ₁	Pirenzepine, 10 nM	Pirenzepine dehydrate, 2 μM	Modified Krebs–buffer (pH 7.4) 5.6 mM KCl, 30.6 mM NaCl, 1.2 mM MgSO ₄ , 1.4 mM KH ₂ PO ₄ , 5.6 mM D–Glucose, 5.2 mM NaHCO ₃ , 2.5 mM CaCl ₂	15 min, 4 °C	60 min, 4 °C	2 × 1 min, 4 °C; 1 s in distilled water
M ₂	Oxotremorine–M, 1.7 nM	Carbachol, 10 μM	20 mM Hepes–Tris (pH 7.5), 10 mM MgCl ₂	20 min, 22 °C	60 min, 22 °C	2 × 2 min, 4 °C; 1 s in distilled water
M ₂	AF–DX 384, 5 nM	Atropine sulfate, 100 μM	Modified Krebs–buffer (pH 7.4) 4.7 mM KCl, 120 mM NaCl, 1.2 mM MgSO ₄ , 1.2 mM KH ₂ PO ₄ , 5.6 mM D–Glucose, 25 mM NaHCO ₃ , 2.5 mM CaCl ₂	15 min, 22 °C	60 min, 22 °C	3 × 4 min, 4 °C; 1 s in distilled water
M ₃	4–DAMP, 1 nM	Atropine sulfate, 10 μM	50 mM Tris–HCl (pH 7.4), 0.1 mM PMSF, 1 mM EDTA	15 min, 22 °C	45 min, 22 °C	2 × 5 min, 4 °C; 1 s in distilled water
Nicotinic	Epibatidine, 0.11 nM	Nicotine, 100 μM	15 mM Hepes (pH 7.5), 120 mM NaCl, 5.4 mM KCl, 0.8 mM MgCl ₂ , 1.8 mM CaCl ₂	20 min, 22 °C	90 min, 4 °C	5 min, 4 °C; 1 s in distilled water
α ₁	Prazosin, 0.09 nM	Phentolamine mesylate, 10 μM	50 mM Na/K-phosphate-buffer (pH 7.4)	15 min, 22 °C	60 min, 22 °C	2 × 5 min, 4 °C; 1 s in distilled water
α ₂	UK14,304, 0.64 nM	Phentolamine mesylate, 10 μM	50 mM Tris–HCl (pH 7.7), 100 μM MnCl ₂	15 min, 22 °C	90 min, 22 °C	5 min, 4 °C; 1 s in distilled water
5-HT _{1A}	8–OH–DPAT, 0.3 nM	5–HT, 1 μM	170 mM Tris–HCl (pH 7.7), 0.01% Ascorbate ^a , 4 mM CaCl ₂ ^a	30 min, 22 °C	60 min, 22 °C	5 min, 4 °C; 3 × 1 s in distilled water
5-HT ₂	Ketanserin, 1.14 nM	Mianserin, 10 μM	170 mM Tris–HCl (pH 7.7)	30 min, 22 °C	120 min, 22 °C	2 × 10 min, 4 °C; 3 × 1 s in distilled water
D ₁	SCH 23390, 1.67 nM	SKF 83566, 1 μM	50 mM Tris–HCl (pH 7.4), 120 mM NaCl, 5 mM KCl, 2 mM CaCl ₂ , 1 mM MgCl ₂ , 1 μM Mianserin ^a	20 min, 22 °C	90 min, 22 °C	2 × 10 min, 4 °C; 1 s in distilled water
D ₂ /D ₃	Raclopride, 0.55 nM	Butaclamol, 1 μM	50 mM Tris–HCl (pH 7.4), 150 mM NaCl, 0.1% Ascorbate	20 min, 22 °C	45 min, 22 °C	6 × 1 min, 4 °C; 1 s in distilled water
D ₂ /D ₃	Fallypride, 4 nM	Haloperidol, 10 μM	50 mM Tris–HCl (pH 7.4), 5 mM KCl, 120 mM NaCl	30 min, 22 °C	60 min, 37 °C	2 × 2 min, 4 °C; 1 s in distilled

(continued on next page)

Table 1 (continued)

Receptor	³ H-ligand, amount in main incubation	Displacer, amount in main incubation	Incubation buffer	Preincubation	Main incubation	Rinsing
A _{2A}	ZM 241385, 0.42 nM	2-Chloro-adenosine, 20 μM	170 mM Tris–HCl (pH 7.4), 1 mM EDTA ^b , 2 U/l Adenosine deaminase ^c , 10 mM MgCl ₂ ^d	30 min, 37 °C prerinsing: 2 × 10 min, 22 °C	120 min, 22 °C	water 2 × 5 min, 4 °C; 1 s in distilled water

^a Main incubation only.

^b Preincubation only.

^c Pre- and main incubation only.

^d Prerinsing and main incubation only.

[³H]prazosin, [³H]UK 14,304, [³H]8-OH-DPAT, [³H]ketanserin, [³H]SCH 23390, [³H]ZM 241385, [³H]fallypride and [³H]raclopride binding.

Films were developed using a Hyperprocessor (Amersham Biosciences, Amersham, UK; now: GE Healthcare Europe GmbH, Freiburg, Germany) and digitized using a CCD-camera (Zeiss, Carl Zeiss Mikrolmaging GmbH, Göttingen, Germany) and the image analyzing software AxioVision (Zeiss, Carl Zeiss Mikrolmaging GmbH, Germany). The co-exposed standards were used to compute non-linear transformations for each film, defining the relationship between gray values in the autoradiograph and concentrations of radioactivity in the tissue (Zilles et al., 2004). Using these transformation curves, the gray value of each pixel was converted into corresponding radioactivity concentrations and subsequently into receptor densities in fmol/mg protein (Zilles et al., 2002a). The resulting linearized images, in which gray values correlate to receptor densities, were contrast-enhanced and color-coded to highlight the regional distribution of the neurotransmitter receptors for visual inspection. For this purpose, a color scale with eleven colors, representing equally spaced gray value ranges, was assigned to the 256 gray values of the linearized autoradiograph.

Statistical analysis

Receptor densities (fmol/mg protein) averaged over all cortical layers were measured using the original, non-contrast-enhanced data sets in eleven different brain regions of interest (ROI), namely the olfactory bulb, the motor, somatosensory, piriform and visual cortices, the striatum, the CA1–3 fields of the hippocampus, the dentate gyrus, the substantia nigra and the cerebellum. For each animal, brain area, and receptor type, three ROIs were measured and averaged, representing the mean binding site density (fmol/mg protein) of a particular animal and area. Data were statistically analyzed for significant differences between control and *Pitx3^{ak}* mice using an analysis of variance (omnibus ANOVA, Systat[®] Version 13). Receptor specific *p*-values < 0.05 were considered statistically significant and followed by tests for each analyzed brain region (post hoc ANOVA). In the case of the cerebellum as

well as the dopamine and adenosine receptor ligands (i.e., SCH 23390 for D₁, raclopride for D₂/D₃, fallypride for D₂/D₃, and ZM 241385 for A₂ receptors), ANOVA was performed for each brain region using post hoc tests with Bonferroni correction.

RESULTS

Using quantitative receptor autoradiography, mean densities (fmol/mg protein) of different receptor binding sites for glutamate, GABA, acetylcholine, noradrenaline, serotonin, dopamine and adenosine were measured in the brains of *Pitx3^{ak}* and control mice. Significant differences were found for eleven receptor types, i.e., kainate, GABA_A, GABA_B, BZ, M₂, M₃, nicotinic, α₁, 5-HT_{1A}, 5-HT₂ and D₂/D₃ (cf. Figs. 1 and 2; Table 2).

In general, the regional distribution pattern of most binding sites, but not the absolute receptor density was similar between *Pitx3^{ak}* and control mice. Thus, the following description of regional receptor distribution refers to both groups, except for the two cases of striatal nicotinic and 5-HT₂ receptors, which will be described separately.

GABA receptor and BZ binding site up-regulation

The most important excitatory and inhibitory neurotransmitter systems of the brain, i.e., glutamate and GABA, were analyzed by measuring AMPA, kainate, NMDA, mGlu2/3, GABA_A and GABA_B receptors as well as GABA_A-associated BZ binding sites.

Mean densities of kainate receptors were similar between most analyzed brain regions, except for the hippocampal CA1 region, the substantia nigra and the cerebellum, where receptor densities were relatively low (cf. Fig. 1). Statistical tests revealed significant differences in kainate receptor densities between *Pitx3^{ak}* and control mice in three ROIs. In the olfactory bulb, the density was decreased by 12% (*p* < 0.05) in the *aphakia* group, while the kainate receptor densities were increased in the striatum and the visual cortex of this group by 11% (*p* < 0.05) and 21% (*p* < 0.01), respectively (cf. Fig. 2; Table 2).

AMPA receptor densities were low in the olfactory bulb, the motor, somatosensory and visual cortex, the striatum,

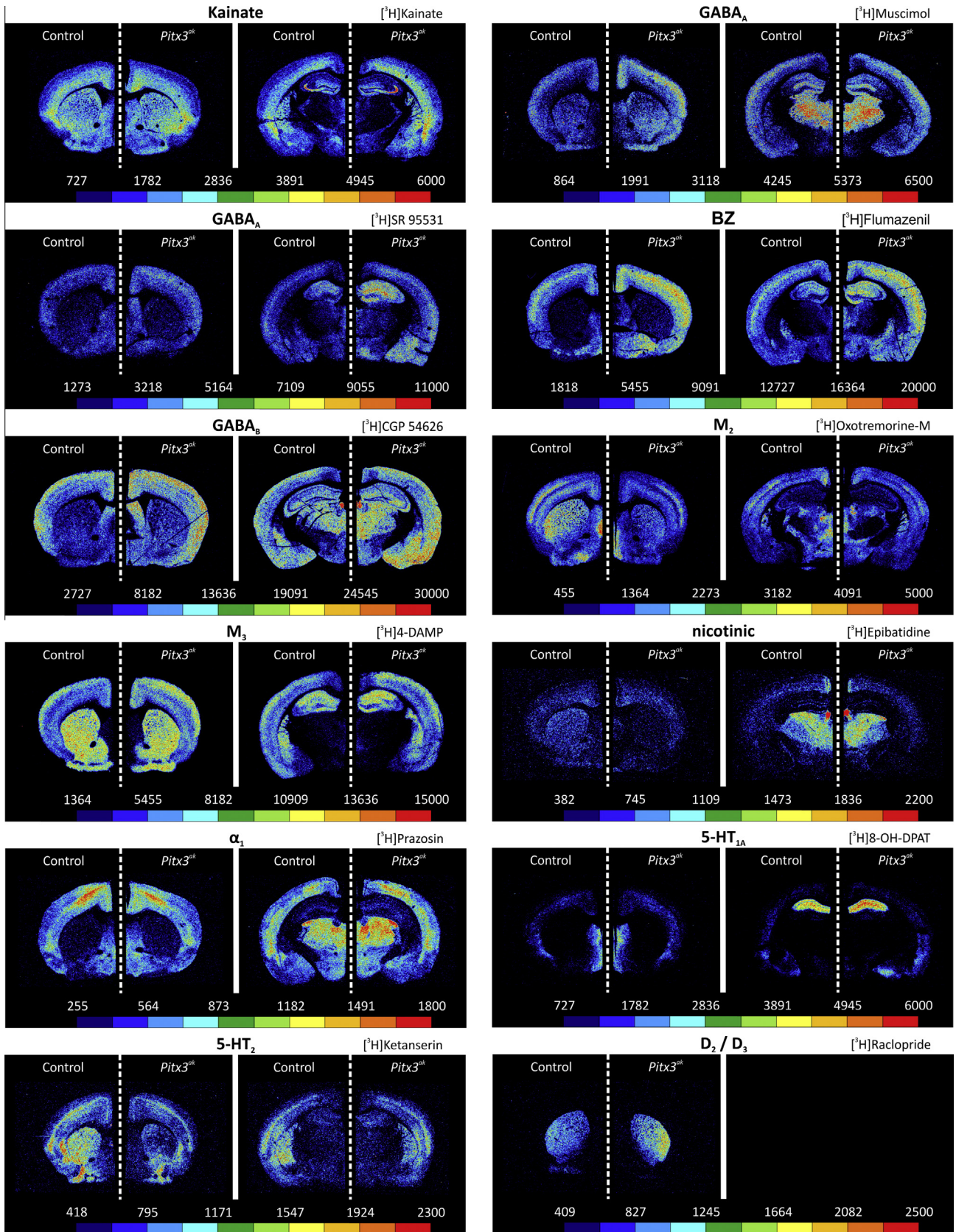


Fig. 1. Contrast-enhanced color-coded images showing the regional distribution of 12 different binding sites within the brains of *Pitx3^{shK}* mice and corresponding control animals (striatal section plane on the left and hippocampal section plane on the right). The assigned color scales with 11 colors representing equally spaced density ranges in fmol/mg protein are shown for each receptor type. Only binding sites that were significantly altered between the two groups are shown. For a complete list of regional receptor densities, see [Table 2](#).

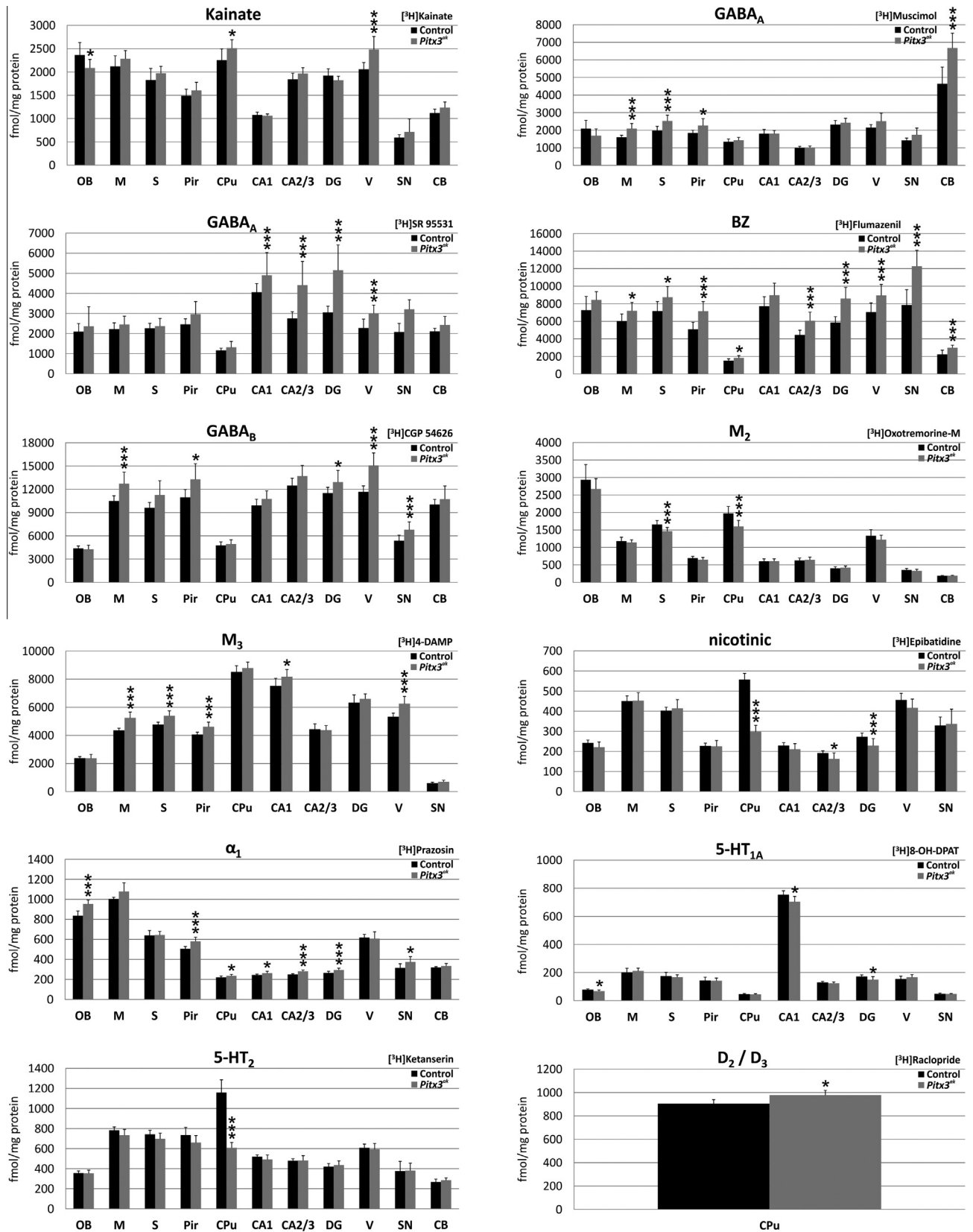


Fig. 2. Mean densities of twelve different binding sites, including standard deviations, in different brain regions of control ($n = 6$; black bars) and *Pitx3*^{3^{ak}} mice ($n = 12$; gray bars). Mean density is indicated as fmol/mg protein. Statistically significant differences are marked by asterisks ($*p < 0.05$ or $***p < 0.01$). Olfactory bulb (OB); motor cortex (M); somatosensory cortex (S); piriform cortex (Pir); caudate putamen (striatum) (CPu); field CA1–3 of hippocampus (CA1–3); dentate gyrus (DG); visual cortex (V); substantia nigra (SN); cerebellum (CB). Only binding sites that were significantly altered between the two groups are shown. For a complete list of regional receptor densities, see [Table 2](#).

Table 2. Mean receptor densities in fmol/mg protein \pm SD measured in different brain regions of control ($n = 6$) and *Pitx3^{shk}* mice ($n = 12$)

Receptor ³ H-ligand	Group	OB	M	S	Pir	CPu	CA1	CA2/3	DG	V	SN	CB
AMPA	Control	447 \pm 104	614 \pm 156	613 \pm 113	1134 \pm 142	590 \pm 175	1663 \pm 524	1304 \pm 425	1252 \pm 367	707 \pm 125	288 \pm 97	328 \pm 61
AMPA	<i>Pitx3^{shk}</i>	396 \pm 84	616 \pm 171	554 \pm 165	1204 \pm 326	496 \pm 130	1605 \pm 634	1220 \pm 421	1152 \pm 391	671 \pm 212	266 \pm 83	295 \pm 76
Kainate	Control	2363 \pm 269	2119 \pm 229	1828 \pm 249	1488 \pm 142	2254 \pm 241	1076 \pm 62	1842 \pm 132	1924 \pm 145	2056 \pm 145	592 \pm 61	1121 \pm 81
Kainate	<i>Pitx3^{shk}</i>	2086 \pm 184*	2284 \pm 175	1972 \pm 15	1605 \pm 172	2513 \pm 179*	1062 \pm 37	1966 \pm 127	1823 \pm 84	2484 \pm 279**	714 \pm 277	1236 \pm 121
NMDA	Control	1332 \pm 83	2225 \pm 74	2236 \pm 48	2350 \pm 134	1493 \pm 60	4751 \pm 247	2820 \pm 152	3713 \pm 207	2454 \pm 62	566 \pm 32	
MK 801	<i>Pitx3^{shk}</i>	1197 \pm 103	2188 \pm 152	2116 \pm 160	2254 \pm 224	1469 \pm 123	4742 \pm 323	2814 \pm 191	3644 \pm 248	2597 \pm 96	473 \pm 78	
mGlu2/3	Control	2817 \pm 396	10692 \pm 1556	11239 \pm 1445	12127 \pm 2231	8956 \pm 2600	4896 \pm 705	3145 \pm 323	8689 \pm 987	12572 \pm 1428	5249 \pm 495	2140 \pm 233
LY 341495	<i>Pitx3^{shk}</i>	3070 \pm 722	11192 \pm 1186	11688 \pm 1436	11904 \pm 1257	8579 \pm 828	4826 \pm 604	3193 \pm 512	8054 \pm 1013	12979 \pm 1676	5924 \pm 1171	2748 \pm 303
GABA _A	Control	2093 \pm 471	1604 \pm 112	1974 \pm 244	1848 \pm 153	1344 \pm 159	1800 \pm 248	994 \pm 88	2319 \pm 236	2151 \pm 172	1422 \pm 136	4641 \pm 951
Muscimol	<i>Pitx3^{shk}</i>	1696 \pm 375	2097 \pm 289**	2526 \pm 337**	2271 \pm 388*	1430 \pm 166	1802 \pm 181	1014 \pm 93	2433 \pm 243	2521 \pm 439	1739 \pm 386	6677 \pm 845**
GABA _A	Control	2098 \pm 403	2228 \pm 305	2262 \pm 247	2460 \pm 273	1165 \pm 105	4057 \pm 431	2750 \pm 334	3052 \pm 310	2276 \pm 443	2081 \pm 422	2104 \pm 152
SR 95531	<i>Pitx3^{shk}</i>	2367 \pm 969	2455 \pm 408	2376 \pm 377	2962 \pm 626	1317 \pm 293	4900 \pm 1135**	4410 \pm 1185**	5159 \pm 1249**	3012 \pm 407**	3210 \pm 474	2431 \pm 423
BZ	Control	7270 \pm 1560	6028 \pm 803	7159 \pm 1078	5101 \pm 788	1531 \pm 191	7730 \pm 1067	4455 \pm 535	5854 \pm 675	7060 \pm 1032	7850 \pm 1752	2225 \pm 493
Flumazenil	<i>Pitx3^{shk}</i>	8438 \pm 937	7195 \pm 951*	8750 \pm 1211*	7142 \pm 1090**	1837 \pm 262*	8976 \pm 1367	6068 \pm 985**	8593 \pm 1262**	8944 \pm 1252**	12284 \pm 1799**	2998 \pm 293**
GABA _B	Control	4373 \pm 305	10491 \pm 675	9620 \pm 676	10969 \pm 1000	4771 \pm 436	9916 \pm 803	12474 \pm 947	11520 \pm 736	11687 \pm 740	5383 \pm 710	10043 \pm 660
CGP 54626	<i>Pitx3^{shk}</i>	4275 \pm 515	12732 \pm 1491**	11271 \pm 1843	13287 \pm 2008*	4933 \pm 555	10774 \pm 1033	13719 \pm 1361	12939 \pm 1495*	15066 \pm 1615**	6784 \pm 1008**	10738 \pm 1682
M ₁	Control	2084 \pm 617	3761 \pm 1052	3785 \pm 1085	4562 \pm 1025	7105 \pm 1868	7136 \pm 1386	3873 \pm 700	7279 \pm 1425	4381 \pm 1494	386 \pm 113	
Pirenzepine	<i>Pitx3^{shk}</i>	1777 \pm 569	3707 \pm 1200	3476 \pm 1079	4366 \pm 1403	5891 \pm 1933	6768 \pm 1917	3507 \pm 980	6400 \pm 1655	4980 \pm 1440	480 \pm 132	
M ₂	Control	2931 \pm 439	1179 \pm 113	1657 \pm 110	694 \pm 50	1976 \pm 197	602 \pm 71	629 \pm 70	402 \pm 47	1332 \pm 177	353 \pm 44	187 \pm 12
Oxotremorine-M	<i>Pitx3^{shk}</i>	2675 \pm 289	1142 \pm 75	1462 \pm 108**	648 \pm 63	1601 \pm 171**	606 \pm 66	644 \pm 78	424 \pm 44	1221 \pm 129	330 \pm 44	188 \pm 14
M ₂	Control	3474 \pm 329	1657 \pm 85	2332 \pm 176	1179 \pm 129	4932 \pm 237	1100 \pm 115	965 \pm 68	705 \pm 38	1951 \pm 229	514 \pm 98	224 \pm 14
AF-DX 384	<i>Pitx3^{shk}</i>	3484 \pm 446	1880 \pm 214	2421 \pm 227	1215 \pm 192	4883 \pm 359	1144 \pm 87	985 \pm 75	765 \pm 53	2137 \pm 249	539 \pm 78	251 \pm 26
M ₃	Control	2383 \pm 105	4355 \pm 154	4766 \pm 170	4060 \pm 164	8507 \pm 439	7518 \pm 549	4440 \pm 378	6336 \pm 545	5336 \pm 250	601 \pm 69	
4-DAMP	<i>Pitx3^{shk}</i>	2379 \pm 267	5252 \pm 407**	5395 \pm 350**	4621 \pm 322**	8799 \pm 412	8180 \pm 504*	4372 \pm 326	6596 \pm 354	6265 \pm 500**	697 \pm 112	
Nicotinic	Control	242 \pm 14	450 \pm 26	403 \pm 17	227 \pm 14	558 \pm 30	229 \pm 14	192 \pm 11	273 \pm 18	456 \pm 33	329 \pm 42	
Epibatidine	<i>Pitx3^{shk}</i>	221 \pm 26	452 \pm 40	415 \pm 43	225 \pm 29	297 \pm 32**	211 \pm 28	163 \pm 30*	229 \pm 34**	417 \pm 43	337 \pm 73	
α_1	Control	837 \pm 47	1004 \pm 16	641 \pm 48	506 \pm 23	221 \pm 14	244 \pm 9	250 \pm 7	265 \pm 17	618 \pm 33	315 \pm 42	320 \pm 8
Prazosin	<i>Pitx3^{shk}</i>	955 \pm 38**	1078 \pm 88	644 \pm 35	582 \pm 41**	236 \pm 14*	263 \pm 18*	282 \pm 12**	294 \pm 17**	608 \pm 68	374 \pm 53*	334 \pm 26
α_2	Control	236 \pm 27	229 \pm 19	226 \pm 26	386 \pm 80	135 \pm 11	269 \pm 27	169 \pm 29	222 \pm 29	264 \pm 20	199 \pm 36	166 \pm 25
UK14,304	<i>Pitx3^{shk}</i>	274 \pm 33	260 \pm 29	239 \pm 28	405 \pm 39	160 \pm 26	266 \pm 32	183 \pm 30	268 \pm 34	298 \pm 53	251 \pm 49	183 \pm 29
5-HT _{1A}	Control	79 \pm 5	202 \pm 29	175 \pm 26	143 \pm 24	47 \pm 4	754 \pm 28	130 \pm 7	172 \pm 12	154 \pm 21	49 \pm 6	
8-OH-DPAT	<i>Pitx3^{shk}</i>	68 \pm 8*	212 \pm 19	168 \pm 17	142 \pm 19	45 \pm 5	704 \pm 38*	124 \pm 9	150 \pm 20*	167 \pm 18	48 \pm 3	
5-HT ₂	Control	357 \pm 21	784 \pm 32	743 \pm 40	735 \pm 77	1159 \pm 127	520 \pm 18	480 \pm 19	421 \pm 31	609 \pm 37	375 \pm 98	268 \pm 29
Ketanserin	<i>Pitx3^{shk}</i>	355 \pm 30	733 \pm 58	699 \pm 55	661 \pm 70	608 \pm 53**	492 \pm 45	482 \pm 47	437 \pm 42	592 \pm 58	381 \pm 74	287 \pm 23
D ₁	Control					4227 \pm 537					1113 \pm 560	
SCH 23390	<i>Pitx3^{shk}</i>					4495 \pm 631					1295 \pm 205	
D ₂ /D ₃	Control					904 \pm 35						
Raclopride	<i>Pitx3^{shk}</i>					977 \pm 42*						
D ₂ /D ₃	Control					2514 \pm 212						
Fallypride	<i>Pitx3^{shk}</i>					2480 \pm 243						
A _{2A}	Control					3265 \pm 364						
ZM 241385	<i>Pitx3^{shk}</i>					3381 \pm 393						

Significant differences are marked by asterisks (* $p < 0.05$ or ** $p < 0.01$). Olfactory bulb (OB); motor cortex (M); somatosensory cortex (S); piriform cortex (Pir); caudate putamen (striatum) (CPu); field CA1–3 of hippocampus (CA1–3); dentate gyrus (DG); visual cortex (V); substantia nigra (SN); cerebellum (CB).

the substantia nigra and the cerebellum. Higher densities were found in the piriform cortex, and particularly, in the hippocampus. No significant differences could be designated in any area between control and *Pitx3^{ak}* animals (cf. Table 2). The NMDA receptors were heterogeneously distributed between the brain regions investigated, showing high receptor densities in the hippocampus, intermediate densities in the motor, somatosensory, piriform and visual cortex and low values in the olfactory bulb, the striatum and the substantia nigra. No significant differences were found between the densities of NMDA receptors in *Pitx3^{ak}* and control mice brains (cf. Table 2). Mean densities of mGlu2/3 receptors were also heterogeneously distributed with high values in the motor, somatosensory, piriform and visual cortex, intermediate densities in the striatum and the dentate gyrus, and low densities in the olfactory bulb, the hippocampal regions CA1 and CA2/3, the substantia nigra and the cerebellum. No significant differences of mGlu2/3 receptor densities were observed between control and *Pitx3^{ak}* mice (cf. Table 2).

GABA_A binding sites revealed by the receptor agonist [³H]muscimol were homogeneously distributed throughout the brain regions investigated, except for a maximum in the cerebellum (cf. Fig. 1). Significantly increased receptor densities were found in the motor (31%; $p < 0.01$), somatosensory (28%; $p < 0.01$) and piriform cortex (23%; $p < 0.05$), as well as in the cerebellum (44%; $p < 0.01$) of *Pitx3^{ak}* mice (cf. Fig. 2; Table 2). Antagonist binding sites revealed by [³H]SR 95531 were more heterogeneously distributed, exhibiting slightly higher densities in the hippocampal regions, low values in the striatum and intermediate densities in the other brain regions (cf. Fig. 1). With this ligand, GABA_A binding site densities were significantly higher in the hippocampus (CA1: 21%; $p < 0.01$; CA2/3: 60%; $p < 0.01$; dentate gyrus: 69%; $p < 0.01$) and the visual cortex (32%; $p < 0.01$) of *Pitx3^{ak}* compared to control mice (cf. Fig. 2; Table 2). Mean densities of GABA_A-associated BZ binding sites were lower in the striatum and the cerebellum, than in the other brain regions investigated (cf. Fig. 1). BZ binding site densities were consistently increased in all investigated brain regions of the *Pitx3^{ak}* group compared to controls. The alterations were statistically significant for most regions, except for the olfactory bulb and CA1, and reached from 19% to 56% (motor cortex, somatosensory cortex, striatum: $p < 0.05$; piriform cortex, visual cortex, CA2/3, dentate gyrus, substantia nigra, cerebellum: $p < 0.01$) (cf. Fig. 2; Table 2). In general, GABA_B receptor densities were high in most ROIs, except for the olfactory bulb, the striatum and the substantia nigra (cf. Fig. 1). Statistical tests showed significant higher receptor densities in the motor (21%; $p < 0.01$), piriform (21%; $p < 0.05$) and visual cortex (29%; $p < 0.01$), the dentate gyrus (12%; $p < 0.05$) and the substantia nigra (26%; $p < 0.01$) of *Pitx3^{ak}* mice (cf. Fig. 2; Table 2).

Striking down-regulation of striatal nicotinic receptors

In the cerebellum, most of the analyzed acetylcholine receptors exhibited densities below the method inherent

detection limit. Mean densities of M₁ receptors were heterogeneously distributed, revealing high values in the striatum, the CA1 region and the dentate gyrus of the hippocampus, low densities in the olfactory bulb and the substantia nigra, and intermediate ones in the other brain regions. There was no significant difference of muscarinic M₁ receptor densities between control mice and *Pitx3^{ak}* mice in the investigated brain regions (cf. Table 2). Muscarinic M₂ receptor densities were high in the olfactory bulb and the striatum (in case of antagonist binding), medium in the motor, somatosensory and visual cortex, and low in all other ROIs (cf. Fig. 1). The distribution of binding sites revealed by either agonist or antagonist binding were similar in most analyzed brain regions, except for the striatal binding site densities, which were higher in case of agonist compared to antagonist binding. Statistical tests revealed significantly decreased M₂ receptor densities in the somatosensory cortex (−12%; $p < 0.01$) as well as in the striatum (−19%; $p < 0.01$) of *Pitx3^{ak}* mice, compared to controls (in case of [³H]oxotremorine-M) (cf. Fig. 2; Table 2). Binding of [³H]AF-DX 384 did not demonstrate significant differences between *Pitx3^{ak}* and control mice (cf. Table 2). Comparable to M₁ receptors, M₃ receptor densities were high in the striatum and CA1, low in the olfactory bulb and particularly in the substantia nigra, and intermediate in the other brain regions (cf. Fig. 1). M₃ receptor densities were significantly increased in all cortical regions of the *Pitx3^{ak}* group, i.e., in the motor (21%; $p < 0.01$), somatosensory (13%; $p < 0.01$), piriform (14%; $p < 0.01$) and visual cortex (17%; $p < 0.01$), as well as in the hippocampal CA1 region (9%; $p < 0.05$) (cf. Fig. 2; Table 2). Mean densities of nicotinic acetylcholine receptors were generally low and similar in most ROI, with slightly higher values in the motor, somatosensory and visual cortex. The control group exhibited a maximum density in the striatum, but *Pitx3^{ak}* mice did not (cf. Fig. 1). Nicotinic acetylcholine receptor densities were significantly decreased by 15% ($p < 0.05$) in the CA2/3 region of the hippocampus, by 16% ($p < 0.01$) in the dentate gyrus, and most prominent by 47% ($p < 0.01$) in the striatum of *Pitx3^{ak}* compared to control animals (cf. Fig. 2; Table 2).

Reductions of serotonergic receptor densities up to 50%

The adrenergic and serotonergic systems were analyzed with regard to α_1 , α_2 , 5-HT_{1A} and 5-HT₂ receptors. The α_1 receptor densities were high in the olfactory bulb and the motor cortex, medium in the somatosensory, piriform and visual cortex, and comparatively low in the other analyzed brain regions (cf. Fig. 1). Statistical tests revealed significantly increased receptor densities in the olfactory bulb (14%; $p < 0.01$), the piriform cortex (15%; $p < 0.01$), the striatum (7%; $p < 0.05$), CA1 (8%; $p < 0.05$), CA2/3 (13%; $p < 0.01$), the dentate gyrus (11%; $p < 0.01$), and the substantia nigra (19%; $p < 0.01$) of *Pitx3^{ak}* mice compared to control animals (cf. Fig. 2; Table 2). In general, the densities of α_2 receptors were low and homogeneously distributed between ROIs, showing slightly higher values in the

piriform cortex. No significant difference between the two groups could be revealed by statistical tests (cf. Table 2). The serotonergic 5-HT_{1A} receptor densities were low in most of the brain regions investigated, except for the CA1 region of the hippocampus, where densities were more than three times higher (cf. Fig. 1). The *Pitx3^{ak}* group showed a significant decrease of 5-HT_{1A} receptor densities in three brain regions, i.e., the olfactory bulb (−13%; $p < 0.05$), CA1 (−7%; $p < 0.05$) and the dentate gyrus (−12%; $p < 0.05$) (cf. Fig. 2; Table 2). Mean densities of 5-HT₂ receptors were low in the olfactory bulb, the hippocampus, the substantia nigra and the cerebellum, whereas densities in the motor, somatosensory, piriform and visual cortex were somewhat higher. In contrast to *Pitx3^{ak}* mice, control mice exhibited a maximum 5-HT₂ receptor density in the striatum (cf. Fig. 1). In this region, receptor density was reduced by nearly half (−48%; $p < 0.01$) in the *Pitx3^{ak}* group (cf. Fig. 2; Table 2).

Dopaminergic D₂/D₃ receptor up-regulation

Mean densities of the dopamine and adenosine receptors investigated were below the method inherent detection limit in the cortical brain regions, but high in the striatum (D₁, D₂/D₃ and A_{2A} receptors) and the substantia nigra (D₁ receptors) (cf. Fig. 1). Statistical tests revealed significantly increased D₂/D₃ receptor densities in the striatum of *Pitx3^{ak}* mice (8%; $p < 0.05$), in case of binding the medium-affinity ligand [³H]raclopride (cf. Fig. 2; Table 2). D₂/D₃ binding site densities revealed by the high-affinity ligand [³H]fallypride, as well as D₁ and A_{2A} receptor densities, did not differ significantly between *Pitx3^{ak}* and control mice in the investigated brain regions (cf. Table 2).

DISCUSSION

We investigated the occurrence of 19 different neurotransmitter receptor binding sites in the brains of *Pitx3^{ak}* mice and control animals by means of quantitative *in vitro* receptor autoradiography. Differential changes were demonstrated for several binding sites of six neurotransmitter systems (i.e., glutamate, GABA, acetylcholine, adrenaline, serotonin and dopamine) (cf. Fig. 2; Table 2). These changes included all regions that we have analyzed (i.e., olfactory bulb; motor, somatosensory, piriform and visual cortices; hippocampal regions CA1, CA2/3 and dentate gyrus; striatum, substantia nigra, and cerebellum).

Pitx3^{ak} mice consistently exhibited a significant increase of GABA_A, GABA_B and BZ binding sites in numerous brain regions (cf. Fig. 2; Table 2). Therefore, these results provide evidence indicating a possible enhancement of cerebral GABA receptor expression in PD. Changes of the GABAergic system were demonstrated in the brains of PD patients, i.e., a significant reduction of cerebral GABA levels (de Jong et al., 1984; Gerlach et al., 1996), while GABA receptor expression has not been investigated so far. Increased GABA binding site densities could be part of a mechanism compensating for reduced GABA levels in PD by receptor

up-regulation. However, further effort is necessary to investigate this issue in detail in *Pitx3^{ak}* as well as in PD-patient brains.

Regarding the acetylcholine system, a striking reduction of nicotinic acetylcholine receptor densities in the hippocampus (15–16% reduction) and striatum (47% reduction) of *Pitx3^{ak}* mice was particularly notable (cf. Fig. 2; Table 2). Similar changes of nicotinic acetylcholine receptors were reported in PD patients concomitant to cognitive or depressive symptoms, respectively (Burghaus et al., 2003; Oishi et al., 2007; Kas et al., 2009; Meyer et al., 2009). Thus, the present data provide further evidence for a correlation between nigrostriatal neurodegeneration and a reduction of nicotinic receptor densities in PD. A neuroprotective effect of nicotine treatment was shown in rats and monkeys after injection of 6-hydroxydopamine (6-OHDA) and 1-methyl-4-phenyl-1,2,3,6-tetrahydropyridin (MPTP), respectively (Costa et al., 2001; Quik et al., 2006; Abin-Carriquiry et al., 2008), while in humans a smoking-related nicotine administration has been associated with a decreased incidence of PD (Allam et al., 2004; Ritz et al., 2007; Noyce et al., 2012).

Adrenergic α_1 receptor densities were significantly increased in different brain regions of *Pitx3^{ak}* mice (cf. Fig. 2; Table 2). This represents an interesting finding since neuronal degeneration has been demonstrated in the locus coeruleus in the brains of PD patients (Bertrand et al., 1997; Zarow et al., 2003), i.e., a major region of noradrenaline synthesis in the brain (Benarroch, 2009). Accordingly, concentrations of noradrenaline were shown to be reduced in PD patients (Scatton et al., 1983; Tohgi et al., 1993). Therefore, increased α_1 receptor densities in different brain regions of *Pitx3^{ak}* mice (cf. Fig. 2; Table 2) may reflect compensatory up-regulations resulting from reduced adrenergic innervation. Our data support the hypothesis that treatment of noradrenergic deficits might complement current dopamine-focused therapeutic approaches, especially with regard to PD-associated depression. For example, the serotonin/noradrenaline reuptake inhibitor venlafaxine was shown to improve depression in PD patients (Richard et al., 2012). Furthermore, the noradrenaline/dopamine reuptake inhibitor bupropion was proposed as treatment of choice in depression associated with PD, avoiding the serotonin-associated side effects of standard medication (Stahl et al., 2004; Raskin and Durst, 2010).

In the present study, serotonergic 5-HT_{1A} receptor densities were significantly decreased in the olfactory bulb and the hippocampal CA1 region of *Pitx3^{ak}* mice compared to control animals, while striatal 5-HT₂ receptor density was massively reduced by nearly 50% (cf. Fig. 2; Table 2). The last is well in line with previous results that revealed a similar down-regulation of 5-HT₂ receptors in 6-OHDA-induced parkinsonian rats (Li et al., 2010). In general, there is a well-described correlation between impairments of the serotonergic system and the occurrence of depression in non-PD patients (Meltzer, 1990; Mann, 1999). However, although depression is a frequent comorbidity of PD (Cummings and Masterman, 1999), to date little is known about the condition of the

serotonergic system in PD patients. Nevertheless, there is some evidence suggesting a PD-related serotonergic affection, e.g. serotonin transporter densities were shown to be reduced in the striatum of PD patients (Kerenyi et al., 2003). Furthermore, 5-HT_{1A} receptor dysfunction was described in PD patients depending on the absence or presence of depression (Ballanger et al., 2012). Thus, our study supplements on the description of PD-associated serotonin receptor changes, supporting current approaches of treating depression as comorbidity of PD via serotonin or dual reuptake inhibitors like paroxetine or nortriptyline (Menza et al., 2009; Richard et al., 2012).

Dopamine D₂/D₃ receptor densities were significantly increased in the striatum of *Pitx3^{ak}* mice compared to control animals (cf. Fig. 2; Table 2). This alteration most likely reflects a compensatory up-regulation induced by the loss of nigrostriatal dopaminergic innervation, a major hallmark of PD as well as of *Pitx3^{ak}* brains (Hwang et al., 2003; Nunes et al., 2003; van den Munckhof et al., 2003; Smidt et al., 2004). These findings are supported by several reports on increased D₂ receptor density in the striatum of PD patients (Rinne et al., 1990a,b; Piggott et al., 1999; Hurley and Jenner, 2006). The fact that binding of [³H]fallypride did not reveal changes in receptor densities comparable to those demonstrated by binding of [³H]raclopride could be ascribed to different receptor affinities of the medium-affinity ligand [³H]raclopride and the high-affinity ligand [³H]fallypride (Stark et al., 2007; Slifstein et al., 2010).

All in all, the striatum is the most influenced brain region in *Pitx3^{ak}* mice, with regard to the number of altered receptors and the magnitude of respective density changes. Kainate, α_1 and D₂/D₃ receptor as well as BZ binding site densities were elevated, while M₂, nicotinic and 5-HT₂ receptor densities were decreased, the latter two by nearly 50% (cf. Fig. 2; Table 2). The striatum is strongly innervated by neurons of the substantia nigra and the function of the nigrostriatal pathway in mice is experimentally accessible via numerous behavioral tests. For example, the challenging beam and the pole test provide sensitive measurements of deficits of the nigrostriatal system (Ogawa et al., 1985; Drucker-Colin and Garcia-Hernandez, 1991; Matsuura et al., 1997). *Pitx3^{ak}* mice exhibit deficits with regard to behavioral tasks sensitive to nigrostriatal dysfunction (Hwang et al., 2005). Hence, the fact that the striatum is the most affected brain region in the present study is in line with the dopaminergic cell loss in the substantia nigra, as well as with the behavioral deficits of *Pitx3^{ak}* mice.

Two more brain regions with differential alterations of neurotransmitter receptor densities are the olfactory bulb and the piriform cortex (cf. Fig. 2; Table 2), which play an important role in olfaction. Odorant molecules are recognized in the olfactory bulb and the information is further analyzed in the piriform cortex, the olfactory tubercle and the amygdala. Olfactory dysfunction is a frequent non-motor symptom of PD (Doty et al., 1988; Hawkes et al., 1997). Impaired olfaction was shown to appear at an early disease stage and can even precede motor symptoms of PD by four years (Ross et al., 2008). Furthermore, an increased risk to develop PD for

people with idiopathic olfactory dysfunction was reported (Ponsen et al., 2004). Changes in neurotransmitter receptor densities, comparable to those described in this study, may underlie the olfactory dysfunction in PD patients. To our knowledge, this issue has not been studied in detail so far and would be an interesting topic to address in the future.

Our results demonstrated differential changes of various receptor densities in the brains of *Pitx3^{ak}* mice. Although PD primarily impairs the dopaminergic system, the receptors of five out of six other neurotransmitter systems studied here showed up- or down-regulations of their densities (i.e., the glutamatergic, GABAergic, cholinergic, adrenergic, and serotonergic systems). Notably, the changes in the dopaminergic system were moderate and limited to a slight increase of D₂/D₃ receptor densities. In contrast, the nicotinic acetylcholine as well as the serotonergic 5-HT₂ receptor densities were massively down-regulated by nearly 50%. Further investigations are necessary to shed light on the detailed cellular mechanisms that are associated with the described receptor density changes.

Moreover, since the *Pitx3^{ak}* mouse represents a developmental model with an early onset of a PD-like phenotype, it would be interesting to compare our results on the altered neurotransmitter receptor densities to other mouse models of PD. One of the most widely used drug-induced animal models of PD is the MPTP-treated mouse, which shows a severe loss of dopaminergic cells caused by the administration of MPTP (Antony et al., 2011; Blesa et al., 2012). In MPTP-treated mice, *Pitx3* is strongly downregulated in the striatum and in the midbrain (Rojas et al., 2012). Recently, it has been shown, that *Pitx3* is expressed selectively in a subpopulation of dopaminergic neurons that are susceptible to neurodegenerative stress caused by application of MPTP (Luk et al., 2013). Therefore, it would be interesting to see whether similar variations of neurotransmitter receptor densities can be observed in this model like those reported here. Since the PD induction in the MPTP model is caused pharmacologically, we expect the pattern and intensity of neurotransmitter receptor changes to vary dependent on the age at injection, the dosage and the time of investigation after injection.

A neurotoxic animal model of PD is generated by the local administration of 6-OHDA (Antony et al., 2011). Since the reduction of striatal 5-HT₂ receptor densities described in our study is in line with previous results that revealed a similar down-regulation in 6-OHDA-induced PD rats (Li et al., 2010), it would be interesting to characterize the other receptors demonstrated to be altered in our study also in the 6-OHDA model. Comparable to MPTP-treated animals, we would expect variations similar to those found in the present study but depending on the parameters of administration.

Based upon the common features of both systems (genetic vs. drug induced), important characteristics for the human PD could be deduced. Actually, some of our findings are in line with findings in brains of PD patients. For example, changes of nicotinic acetylcholine

receptors were reported in PD patients (Burghaus et al., 2003; Oishi et al., 2007; Kas et al., 2009), 5-HT_{1A} receptor dysfunction was described in PD patients depending on the absence or presence of depression (Ballanger et al., 2012) and D₂ receptor densities were also shown to be increased in PD patients (Rinne et al., 1990a,b; Hurley and Jenner, 2006).

Taken together, we here presented novel data on the expression of various neurotransmitter receptors in the brains of *Pitx3^{ak}* mice, a mouse model exhibiting neuropathological, behavioral and pharmacological features of PD. The impact of non-dopaminergic systems in the molecular pathology of PD is highlighted by the present observations, pointing to new targets for pharmaceutical intervention.

Acknowledgment—We thank Dr. V. Derdau (Sanofi-Aventis, Frankfurt, Germany) for his assistance in the purification of [³H]fallypride.

REFERENCES

- Abin-Carriquiry JA, Costa G, Urbanavicius J, Cassels BK, Rebolledo-Fuentes M, Wonnacott S, Dajas F (2008) In vivo modulation of dopaminergic nigrostriatal pathways by cytosine derivatives: implications for Parkinson's Disease. *Eur J Pharmacol* 589:80–84.
- Ahmad N, Aslam M, Muenster D, Horsch M, Khan MA, Carlsson P, Beckers J, Graw J (2013) *Pitx3* directly regulates *Foxe3* during early lens development. *Int J Dev Biol* 57:741–751.
- Allam MF, Campbell MJ, Hofman A, Del Castillo AS, Fernandez-Crehuet Navajas R (2004) Smoking and Parkinson's disease: systematic review of prospective studies. *Mov Disord* 19:614–621.
- Antony PM, Diederich NJ, Balling R (2011) Parkinson's disease mouse models in translational research. *Mamm Genome* 22:401–419.
- Ardayfio P, Moon J, Leung KK, Youn-Hwang D, Kim KS (2008) Impaired learning and memory in *Pitx3* deficient aphakia mice: a genetic model for striatum-dependent cognitive symptoms in Parkinson's disease. *Neurobiol Dis* 31:406–412.
- Ballanger B, Klinger H, Eche J, Lerond J, Vallet AE, Le Bars D, Tremblay L, Sgambato-Faure V, Broussolle E, Thobois S (2012) Role of serotonergic 1A receptor dysfunction in depression associated with Parkinson's disease. *Mov Disord* 27:84–89.
- Benarroch EE (2009) The locus ceruleus norepinephrine system: functional organization and potential clinical significance. *Neurology* 73:1699–1704.
- Bertrand E, Lechowicz W, Szpak GM, Dymecki J (1997) Qualitative and quantitative analysis of locus coeruleus neurons in Parkinson's disease. *Folia Neuropathol* 35:80–86.
- Blesa J, Phani S, Jackson-Lewis V, Przedborski S (2012) Classic and new animal models of Parkinson's disease. *J Biomed Biotechnol*. <http://dx.doi.org/10.1155/2012/845618>.
- Burghaus L, Schutz U, Krempel U, Lindstrom J, Schroder H (2003) Loss of nicotinic acetylcholine receptor subunits alpha4 and alpha7 in the cerebral cortex of Parkinson patients. *Parkinsonism Relat Disord* 9:243–246.
- Costa G, Abin-Carriquiry JA, Dajas F (2001) Nicotine prevents striatal dopamine loss produced by 6-hydroxydopamine lesion in the substantia nigra. *Brain Res* 888:336–342.
- Cremer C, Lübke JR, Palomero-Gallagher N, Zilles K (2011) Laminar distribution of neurotransmitter receptors in different reeler mouse brain regions. *Brain Struct Funct* 216:201–218.
- Cremer CM, Palomero-Gallagher N, Bidmon HJ, Schleicher A, Speckmann EJ, Zilles K (2009) Pentylentetrazole-induced seizures affect binding site densities for GABA, glutamate and adenosine receptors in the rat brain. *Neuroscience* 163:490–499.
- Cummings JL, Masterman DL (1999) Depression in patients with Parkinson's disease. *Int J Geriatr Psychiatry* 14:711–718.
- de Jong PJ, Lakke JP, Teelken AW (1984) CSF GABA levels in Parkinson's disease. *Adv Neurol* 40:427–430.
- Ding Y, Restrepo J, Won L, Hwang DY, Kim KS, Kang UJ (2007) Chronic 3,4-dihydroxyphenylalanine treatment induces dyskinesia in aphakia mice, a novel genetic model of Parkinson's disease. *Neurobiol Dis* 27:11–23.
- Doty RL, Deems DA, Stellar S (1988) Olfactory dysfunction in parkinsonism: a general deficit unrelated to neurologic signs, disease stage, or disease duration. *Neurology* 38:1237–1244.
- Drucker-Colin R, Garcia-Hernandez F (1991) A new motor test sensitive to aging and dopaminergic function. *J Neurosci Methods* 39:153–161.
- Gerlach M, Gsell W, Kornhuber J, Jellinger K, Krieger V, Pantucek F, Vock R, Riederer P (1996) A post mortem study on neurochemical markers of dopaminergic, GABA-ergic and glutamatergic neurons in basal ganglia-thalamocortical circuits in Parkinson syndrome. *Brain Res* 741:142–152.
- Graw J (1999) Cataract mutations and lens development. *Prog Retin Eye Res* 18:235–267.
- Grimm C, Chatterjee B, Favor J, Immervoll T, Loster J, Klopp N, Sandulache R, Graw J (1998) Aphakia (ak), a mouse mutation affecting early eye development: fine mapping, consideration of candidate genes and altered *Pax6* and *Six3* gene expression pattern. *Dev Genet* 23:299–316.
- Hawkes CH, Shephard BC, Daniel SE (1997) Olfactory dysfunction in Parkinson's disease. *J Neurol Neurosurg Psychiatry* 62:436–446.
- Hurley MJ, Jenner P (2006) What has been learnt from study of dopamine receptors in Parkinson's disease? *Pharmacol Ther* 111:715–728.
- Hwang DY, Ardayfio P, Kang UJ, Semina EV, Kim KS (2003) Selective loss of dopaminergic neurons in the substantia nigra of *Pitx3*-deficient aphakia mice. *Brain Res Mol Brain Res* 114:123–131.
- Hwang DY, Fleming SM, Ardayfio P, Moran-Gates T, Kim H, Tarazi FI, Chesselet MF, Kim KS (2005) 3,4-Dihydroxyphenylalanine reverses the motor deficits in *Pitx3*-deficient aphakia mice: behavioral characterization of a novel genetic model of Parkinson's disease. *J Neurosci* 25:2132–2137.
- Kas A, Bottlaender M, Gallezot JD, Vidailhet M, Villafane G, Gregoire MC, Coulon C, Valette H, Dolle F, Ribeiro M-J, Hantraye P, Remy P (2009) Decrease of nicotinic receptors in the nigrostriatal system in Parkinson's disease. *J Cereb Blood Flow Metab* 29:1601–1608.
- Kerenyi L, Ricaurte GA, Schretlen DJ, McCann U, Varga J, Mathews WB, Ravert HT, Dannals RF, Hilton J, Wong DF, Szabo Z (2003) Positron emission tomography of striatal serotonin transporters in Parkinson disease. *Arch Neurol* 60:1223–1229.
- Li Y, Huang XF, Deng C, Meyer B, Wu A, Yu Y, Ying W, Yang GY, Yenari MA, Wang Q (2010) Alterations in 5-HT_{2A} receptor binding in various brain regions among 6-hydroxydopamine-induced Parkinsonian rats. *Synapse* 64:224–230.
- Lohle M, Storch A, Reichmann H (2009) Beyond tremor and rigidity: non-motor features of Parkinson's disease. *J Neural Transm* 116:1483–1492.
- Luk KC, Rymar VV, van den Munckhof P, Nicolau S, Steriade C, Bifsha P, Drouin J, Sadikot AF (2013) The transcription factor *Pitx3* is expressed selectively in midbrain dopaminergic neurons susceptible to neurodegenerative stress. *J Neurochem* 125:932–943.
- Mann JJ (1999) Role of the serotonergic system in the pathogenesis of major depression and suicidal behavior. *Neuropsychopharmacology* 21:99S–105S.
- Matsuura K, Kabuto H, Makino H, Ogawa N (1997) Pole test is a useful method for evaluating the mouse movement disorder caused by striatal dopamine depletion. *J Neurosci Methods* 73:45–48.

- Meltzer HY (1990) Role of serotonin in depression. *Ann N Y Acad Sci* 600:486–499.
- Menza M, Dobkin RD, Marin H, Mark MH, Gara M, Buyske S, Bienfait K, Dicke A (2009) A controlled trial of antidepressants in patients with Parkinson disease and depression. *Neurology* 72:886–892.
- Meyer PM, Strecker K, Kendziorra K, Becker G, Hesse S, Woelpl D, Hensel A, Patt M, Sorger D, Wegner F, Lobsien D, Barthel H, Brust P, Gertz HJ, Sabri O, Schwarz J (2009) Reduced $\alpha 4\beta 2$ -nicotinic acetylcholine receptor binding and its relationship to mild cognitive and depressive symptoms in Parkinson disease. *Arch Gen Psychiatry* 66:866–877.
- Noyce AJ, Bestwick JP, Silveira-Moriyama L, Hawkes CH, Giovannoni G, Lees AJ, Schrag A (2012) Meta-analysis of early nonmotor features and risk factors for Parkinson disease. *Ann Neurol* 72:893–901.
- Nunes I, Tovmasian LT, Silva RM, Burke RE, Goff SP (2003) Pitx3 is required for development of substantia nigra dopaminergic neurons. *Proc Natl Acad Sci U S A* 100:4245–4250.
- Oermann E, Warskulat U, Heller-Stilb B, Häussinger D, Zilles K (2005) Taurine-transporter gene knockout-induced changes in GABAA, kainate and AMPA but not NMDA receptor binding in mouse brain. *Anat Embryol* 210:363–372.
- Ogawa N, Hirose Y, Ohara S, Ono T, Watanabe Y (1985) A simple quantitative bradykinesia test in MPTP-treated mice. *Res Commun Chem Pathol Pharmacol* 50:435–441.
- Oishi N, Hashikawa K, Yoshida H, Ishizu K, Ueda M, Kawashima H, Saji H, Fukuyama H (2007) Quantification of nicotinic acetylcholine receptors in Parkinson's disease with (123)I-5IA SPECT. *J Neuro Sci* 256:52–60.
- Palomero-Gallagher N, Bidmon HJ, Cremer M, Schleicher A, Kircheis G, Reifensberger G, Kostopoulos G, Haussinger D, Zilles K (2009) Neurotransmitter receptor imbalances in motor cortex and basal ganglia in hepatic encephalopathy. *Cell Physiol Biochem* 24:291–306.
- Palomero-Gallagher N, Bidmon HJ, Zilles K (2003) AMPA, kainate, and NMDA receptor densities in the hippocampus of untreated male rats and females in estrus and diestrus. *J Comp Neurol* 459:468–474.
- Palomero-Gallagher N, Schleicher A, Bidmon HJ, Pannek HW, Hans V, Gorji A, Speckmann EJ, Zilles K (2012) Multireceptor analysis in human neocortex reveals complex alterations of receptor ligand binding in focal epilepsies. *Epilepsia* 53:1987–1997.
- Park A, Stacy M (2009) Non-motor symptoms in Parkinson's disease. *J Neurol* 3:293–298.
- Piggott MA, Marshall EF, Thomas N, Lloyd S, Court JA, Jaros E, Burn D, Johnson M, Perry RH, McKeith IG, Ballard C, Perry EK (1999) Striatal dopaminergic markers in dementia with Lewy bodies, Alzheimer's and Parkinson's diseases: rostrocaudal distribution. *Brain* 122(Pt 8):1449–1468.
- Ponsen MM, Stoffers D, Booij J, van Eck-Smit BL, Wolters E, Berendse HW (2004) Idiopathic hyposmia as a preclinical sign of Parkinson's disease. *Ann Neurol* 56:173–181.
- Quik M, Parameswaran N, McCallum SE, Bordia T, Bao S, McCormack A, Kim A, Tyndale RF, Langston JW, Di Monte DA (2006) Chronic oral nicotine treatment protects against striatal degeneration in MPTP-treated primates. *J Neurochem* 98:1866–1875.
- Raskin S, Durst R (2010) Bupropion as the treatment of choice in depression associated with Parkinson's disease and its various treatments. *Med Hypotheses* 75:544–546.
- Richard IH et al (2012) A randomized, double-blind, placebo-controlled trial of antidepressants in Parkinson disease. *Neurology* 78:1229–1236.
- Rieger DK, Reichenberger E, McLean W, Sidow A, Olsen BR (2001) A double-deletion mutation in the Pitx3 gene causes arrested lens development in aphakia mice. *Genomics* 72:61–72.
- Rinne JO, Laihininen A, Nagren K, Bergman J, Solin O, Haaparanta M, Ruotsalainen U, Rinne UK (1990a) PET demonstrates different behaviour of striatal dopamine D-1 and D-2 receptors in early Parkinson's disease. *J Neurosci Res* 27:494–499.
- Rinne UK, Laihininen A, Rinne JO, Nagren K, Bergman J, Ruotsalainen U (1990b) Positron emission tomography demonstrates dopamine D2 receptor supersensitivity in the striatum of patients with early Parkinson's disease. *Mov Disord* 5:55–59.
- Ritz B, Ascherio A, Checkoway H, Marder KS, Nelson LM, Rocca WA, Ross GW, Strickland D, Van Den Eeden SK, Gorell J (2007) Pooled analysis of tobacco use and risk of Parkinson disease. *Arch Neurol* 64:990–997.
- Rodriguez MC, Obeso JA, Olanow CW (1998) Subthalamic nucleus-mediated excitotoxicity in Parkinson's disease: a target for neuroprotection. *Ann Neurol* 44:S175–188.
- Rojas P, Ruiz-Sánchez E, Rojas C, Ögren SO (2012) Ginkgo biloba extract (EGb 761) modulates the expression of dopamine-related genes in 1-methyl-4-phenyl-1,2,3,6-tetrahydropyridine-induced Parkinsonism in mice. *Neuroscience* 223:246–257.
- Ross GW, Petrovitch H, Abbott RD, Tanner CM, Popper J, Masaki K, Launer L, White LR (2008) Association of olfactory dysfunction with risk for future Parkinson's disease. *Ann Neurol* 63:167–173.
- Scatton B, Javoy-Agid F, Rouquier L, Dubois B, Agid Y (1983) Reduction of cortical dopamine, noradrenaline, serotonin and their metabolites in Parkinson's disease. *Brain Res* 275:321–328.
- Semina EV, Murray JC, Reiter R, Hrstka RF, Graw J (2000) Deletion in the promoter region and altered expression of Pitx3 homeobox gene in aphakia mice. *Hum Mol Genet* 9:1575–1585.
- Slifstein M, Kegeles LS, Xu X, Thompson JL, Urban N, Castrillon J, Hackett E, Bae S-A, Laruelle M, Abi-Dargham A (2010) Striatal and extrastriatal dopamine release measured with PET and [18F]fallypride. *Synapse* 64:350–362.
- Smidt MP, Smits SM, Bouwmeester H, Hamers FP, van der Linden AJ, Hellemons AJ, Graw J, Burbach JP (2004) Early developmental failure of substantia nigra dopamine neurons in mice lacking the homeodomain gene Pitx3. *Development* 131:1145–1155.
- Stahl SM, Pradko JF, Haight BR, Modell JG, Rockett CB, Learned-Coughlin S (2004) A review of the neuropharmacology of bupropion, a dual norepinephrine and dopamine reuptake inhibitor. *Prim Care Companion J Clin Psychiatry* 6:159–166.
- Stark D, Piel M, Hübner H, Gmeiner P, Gründer G, Rösch F (2007) In vitro affinities of various halogenated benzamide derivatives as potential radioligands for non-invasive quantification of D2-like dopamine receptors. *Bioorg Med Chem* 15:6819–6829.
- Tohgi H, Abe T, Takahashi S, Takahashi J, Nozaki Y, Ueno M, Kikuchi T (1993) Monoamine metabolism in the cerebrospinal fluid in Parkinson's disease: relationship to clinical symptoms and subsequent therapeutic outcomes. *J Neural Transm Park Dis Dement Sect* 5:17–26.
- van den Munckhof P, Gilbert F, Chamberland M, Levesque D, Drouin J (2006) Striatal neuroadaptation and rescue of locomotor deficit by L-DOPA in aphakia mice, a model of Parkinson's disease. *J Neurochem* 96:160–170.
- van den Munckhof P, Luk KC, Ste-Marie L, Montgomery J, Blanchet PJ, Sadikot AF, Drouin J (2003) Pitx3 is required for motor activity and for survival of a subset of midbrain dopaminergic neurons. *Development* 130:2535–2542.
- Varani K, Vincenzi F, Tosi A, Gessi S, Casetta I, Granieri G, Fazio P, Leung E, MacLennan S, Granieri E, Borea PA (2010) A2A adenosine receptor overexpression and functionality, as well as TNF-alpha levels, correlate with motor symptoms in Parkinson's disease. *FASEB J* 24:587–598.
- Zarow C, Lyness SA, Mortimer JA, Chui HC (2003) Neuronal loss is greater in the locus coeruleus than nucleus basalis and substantia nigra in Alzheimer and Parkinson diseases. *Arch Neurol* 60:337–341.
- Ziemssen T, Reichmann H (2007) Non-motor dysfunction in Parkinson's disease. *Parkinsonism Relat Disord* 13:323–332.
- Zilles K, Qu MS, Kohling R, Speckmann EJ (1999) Ionotropic glutamate and GABA receptors in human epileptic neocortical tissue: quantitative in vitro receptor autoradiography. *Neuroscience* 94:1051–1061.
- Zilles K, Wu J, Crusio WE, Schwegler H (2000) Water maze and radial maze learning and the density of binding sites of glutamate, GABA, and serotonin receptors in the hippocampus of inbred mouse strains. *Hippocampus* 10:213–225.

Zilles K, Schleicher A, Palomero-Gallagher N, Amunts K (2002a) Quantitative analysis of cyto- and receptor architecture of the human brain. In: Toga AW, Mazziotta JC, editors. Brain mapping: the methods. Elsevier Inc. p. 573–602.

Zilles K, Palomero-Gallagher N, Grefkes C, Scheperjans F, Boy C, Amunts K, Schleicher A (2002b) Architectonics of the human

cerebral cortex and transmitter receptor fingerprints: reconciling functional neuroanatomy and neurochemistry. Eur Neuropsychopharmacol 12:587–599.

Zilles K, Palomero-Gallagher N, Schleicher A (2004) Transmitter receptors and functional anatomy of the cerebral cortex. J Anat 205:417–432.

(Accepted 22 October 2014)
(Available online 5 November 2014)